

Journal of Materials Chemistry C

Accepted Manuscript



This is an *Accepted Manuscript*, which has been through the Royal Society of Chemistry peer review process and has been accepted for publication.

Accepted Manuscripts are published online shortly after acceptance, before technical editing, formatting and proof reading. Using this free service, authors can make their results available to the community, in citable form, before we publish the edited article. We will replace this *Accepted Manuscript* with the edited and formatted *Advance Article* as soon as it is available.

You can find more information about *Accepted Manuscripts* in the [Information for Authors](#).

Please note that technical editing may introduce minor changes to the text and/or graphics, which may alter content. The journal's standard [Terms & Conditions](#) and the [Ethical guidelines](#) still apply. In no event shall the Royal Society of Chemistry be held responsible for any errors or omissions in this *Accepted Manuscript* or any consequences arising from the use of any information it contains.

Cite this: DOI: 10.1039/c0xx00000x

PAPER

www.rsc.org/MaterialsC

New Homoleptic Iridium Complexes with C[^]N=N Type Ligand for High Efficiency Orange and Single Emissive-layer White OLEDs

Li Yuan Guo,^{†a} Xun Lu Zhang,^{†a} Hai Shan Wang,^a Chen Liu,^a Zhi Gang Li,^b Zhang Jin Liao,^b Bao Xiu Mi,^{*a} Xin Hui Zhou,^b Chao Zheng,^a Yong Hua Li^a and Zhi Qiang Gao^{*b}⁵ Received (in XXX, XXX) Xth XXXXXXXXX 20XX, Accepted Xth XXXXXXXXX 20XX

DOI: 10.1039/b000000x

In this paper, we developed two new strong orange-emission and thermally stable iridium complexes, IrCzPPya {tris[9-(6-phenylpyridazin-3-yl)-9H-carbazole] iridium(III)} and IrNPPya [tris(N,N,6-triphenylpyridazin-3-amine) iridium(III)] by introducing hole transporting moiety to the C[^]N=N type ligand, i.e. carbazole and diphenylamine. Based on experimental results plus quantum chemistry calculations, the link between molecular structures and material properties was demonstrated. Using IrNPPya as the dopant emitter, the organic light-emitting device (OLED) showed extremely high efficiency of 70.8 cd A⁻¹ (75.4 lm W⁻¹, 30.8%) with wavelength up to 560 nm. More importantly, the efficiency was still as high as 63.3 cd A⁻¹ (43.5 lm W⁻¹, 21.8%) at a brightness of 1000 cd m⁻², showing very low efficiency roll-off. By combining IrNPPya with the blue emitter FIrpic [bis(4,6-difluorophenyl-pyridinato-N,C2['])(picolinate) iridium(III)], a single emissive-layer white OLED (WOLED) with high efficiency and good Commission Internationale de l'Eclairage (CIE) coordinates has been successfully constructed. The device achieved maximum efficiencies of 55.9 lm W⁻¹, 49.9 cd A⁻¹, and 23.9% with CIE coordinates of (0.33, 0.46), which are among the best with similar CIE coordinates. The strategies for obtaining high efficiency WOLED with simple three organic layers were highlighted.

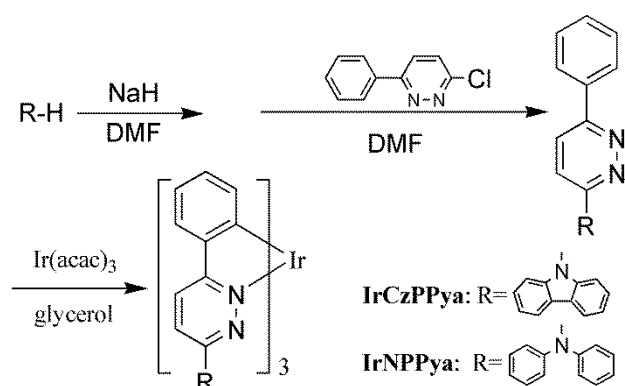
1 Introduction

Organic light-emitting diodes (OLEDs) have realized flat-panel-displays (FPD) for both small and large sizes, and are heading for high efficiency and low voltage white OLEDs (WOLEDs) mainly aiming at energy-saving and feeling-pleasant solid-state lighting (SSL).¹⁻³ Compared to fluorescent materials, phosphorescent-emitter based OLEDs (PhOLEDs) are superior because they can harvest both singlet and triplet exciton to achieve internal quantum efficiencies (IQEs) of nearly 100%,⁴ enabling high external quantum efficiencies (EQEs) of roughly 20-30%.⁵⁻⁷ Even though various colors of phosphorescent Ir(III) complexes can be prepared by varying the structure of the ligands,^{6,9} the design and synthesis of efficient orange phosphorescent complexes have attracted more research interest, since orange phosphor is a key parameter in WOLEDs with complimentary color scheme. Recently, Liu et al. reported an efficient WOLED comprising a strong yellow emitter with wavelength of 566 nm based on ligand of 2-aryl-benzothiazole. The maximum efficiencies of the yellow and WOLED devices are 58.4 cd A⁻¹ (49.7 lm W⁻¹) and 26.6 cd A⁻¹ (14.5 lm W⁻¹) respectively.¹⁰ Later, Cheng et al. developed low-efficiency roll-off and color stability WOLEDs using new orange iridium(III) complex (dpiq)₂Ir(acac), exhibiting high efficiencies of 68.8 cd A⁻¹ and 45.0 lm W⁻¹ with Commission Internationale de l'Eclairage (CIE) coordinates of (0.44, 0.45).¹¹ Sun et al. prepared high-color-rendering WOLEDs with a wide-bandwidth orange iridium(III) complex (pbi)₂Ir(biq), exhibiting a high CRI of 80 and a peak efficiencies of 22.1 cd A⁻¹ and 25.5

lm W⁻¹.¹² Xie et al. reported very high efficiency solution-processed all-phosphor-doped WOLEDs based on a newly developed dendrimer host and a novel orange iridium complex. The solution-processed WOLEDs showed a forward-viewing efficiencies of 70.6 cd A⁻¹, 47.6 lm W⁻¹ and 26% at a luminance of 100 cd m⁻².¹³

Although great achievements have been made, there are still several problems. On one hand, it is still difficult to simultaneously achieve an outstanding efficiency and good CIE coordinates in white OLED. On the other hand, some of the structures of the WOLEDs comprise several emitting layers (EMLs), complicating device fabrication. Therefore, developing high efficient orange electroluminescence (EL) and corresponding WOLEDs with single EML are still interesting.

Previously, we have reported iridium complexes with ligand bearing C[^]N=N [e.g., 3,6-Bis(phenyl)pyridazine (HBPPya)] structure for OLEDs, in which the chelating N is adjacent to a sp² N atom without H attachment.^{9,14-16} The advantage of the C[^]N=N type ligand lies in the fact that due to the lack of H atom in vicinity to the chelating N atom (i.e., pyridine vs pyridazine), steric hindrance between N and Ir is small, resulting in stronger N-Ir bonding, and hence robust iridium complexes with intensive phosphorescence. These prominent features have been confirmed by both experimental works and theoretical studies from other groups.¹⁷⁻²⁰ However, as a new type of iridium complexes, their usages in WOLEDs have been rarely reported, mainly because of the lack of strong and suitable yellow/orange emitters of this type.¹⁹ Recently, using our previously reported C[^]N=N ligand



Scheme 1. Synthetic routes for IrCzPPya and IrNPPya

of HBPPya and combining with acetyl acetone, a heteroleptic iridium complex $[(\text{Bppy})_2\text{Ir}(\text{acac})]$ with promising orange electroluminescence (EL) and satisfactory white EL was reported by us.²¹

In this work, we developed two new $\text{C}^{\wedge}\text{N}=\text{N}$ type ligands with hole transporting moiety of carbazole and diphenylamine, and two new homoleptic tricyclic metalated iridium complexes with strong orange emission, i.e., tris[9-(6-phenylpyridazin-3-yl)-9H-carbazole] iridium(III) (IrCzPPya) and tris(N,N,6-triphenylpyridazin-3-amine) iridium(III) (IrNPPya). Using IrNPPya as the dopant emitter, orange EL with ultra-high EQE above 30% was achieved, which are among the best data for the orange OLEDs reported so far. Furthermore, employing quadrilaminar single EML comprising the orange phosphor IrNPPya and the traditional blue phosphor FIrpic [bis(4,6-difluorophenyl)pyridinato-N,C2'] (picolinate) iridium(III)], as well the cohost of TCTA [4,4',4''-tri(N-carbazolyl)triphenylamine] and BmPyPB [1,3-bis(3,5-dipyrid-3-yl-phenyl)benzene],²² high efficiency WOLED was realized, with CIE coordinates of (0.33, 0.46) at 1000 cd m^{-2} , and peak forward viewing efficiencies of 55.9 lm W^{-1} , 49.9 cd A^{-1} , and 23.9%. These are among the highest efficiencies reported to date for two-element all-phosphor WOLEDs employing a single EML with similar CIE coordinates.²³

2 Experimental

2.1 Instrumentation and synthesis

Absorption spectra of solutions ($\sim 1.0 \times 10^{-5}$ M in DCM) were recorded with Shimadzu UV-3600 spectrophotometer from 200 to 600 nm. Photoluminescence (PL) spectra were measured in DCM ($\sim 1.0 \times 10^{-5}$ M) using a Shimadzu RF-5301PC spectrofluorophotometer in the range of 400–700 nm. Fluorescence quantum yields were determined in the DCM solution at 298 K with Ir(ppy)₃ as a standard. The absorbance at excitation wavelength was kept below 0.05 for the samples and the standard. Electron ionization (EI) mass spectrum (MS) was recorded on a Shimadzu GCMS-QP2010 PLUS mass spectrometer, or on a Bruker matrix-assisted laser desorption/ionization time-of-flight (MALDI-TOF). Thermal gravimetric analysis was performed on a Shimadzu Thermogravimetric Analyzer DTG-60. The samples were heated at a heating rate of 10 $^{\circ}\text{C min}^{-1}$. Elemental analysis of carbon,

hydrogen, and nitrogen was performed on a Vario EL microanalyzer. Electrochemical analysis was performed on a Bioanalytical Systems CHI660E operating in cyclic voltammetry (CV) mode. A three-electrode system consisting of glass carbon and platinum wire as working and auxiliary electrodes, and an Ag/AgCl as reference electrode was used. The scan rate was 100 mV/s. Tetrabutylammonium perchlorate (0.1 M) in DCM was used as a supporting electrolyte. HOMOs were obtained using the equation: $E_{\text{HOMO}} = 4.71 + E_{\text{OX}}$ (eV), while LUMOs were obtained via HOMO minus the energy gap of the triplet absorption cutoff from absorption spectra. ¹H NMR spectra were recorded with a Bruker Ultra Shield Plus 400 MHz spectrometer. Transient fluorescence study was performed with an Edinburgh Instruments FLS920 spectrometer. Samples were prepared and degassed in the same way as described for steady state photoluminescence measurements. A hydrogen-filled/or a nitrogen lamp was used as an excitation source and a red-sensitive (185–850 nm) Hamamatsu R-3237-01 photomultiplier tube as a detector. The data were fitted to single-exponential functions of the form $I(t) = I_0 \exp(-t/\tau)$. Quantum chemistry calculations were performed using the B3LYP hybrid functional in Gaussian 03 programs. The “double- ξ ” quality basis set LANL2DZ associated with the pseudopotential was employed on atom Ir. The 6-31G(d) basis set was used for nonmetal atoms.

The synthetic routes for the titled complexes are described in Scheme 1. After ligand synthesis according to the literature,²⁴ IrCzPPya and IrNPPya were prepared by a well known method with moderate yield.^{25,26} They were then purified by column chromatography and characterized by ¹H and ¹³C NMR spectroscopy, mass spectrometry (MS) and elemental analyses, fully confirming their molecular structures. Being an octahedral geometry, these complexes might be facial or/and meridional isomer(s). From the ¹H NMR spectrum (Fig. S1 and S2), it can be seen that in both complexes of IrCzPPya and IrNPPya, the number of resonances in each complex are equal to those in a single anionic $\text{C}^{\wedge}\text{N}=\text{N}$ ligand, confirming that these complexes are pure facial isomers.²⁷

2.1.1 Synthesis of 9-(6-Phenyl-pyridazin-3-yl)-9H-carbazole (HCzPPya)

All reagents and solvents were obtained from commercial suppliers and used as received. Carbazole (1.67 g, 1 mol) was dissolved in anhydrous dimethylformamide (DMF) (20 mL) under nitrogen, and stirred. NaH (60%, 0.709 g, 0.03 mol) was added to the solution in small portions within 10 min, avoiding vigorous bubbling and heating. After stirring for 1 h at room temperature, and then, 3-chloro-6-phenyl-pyridazine (1.34 g, 0.7 mol), bought from commercial supplier of J&K, was dissolved in DMF (50 mL) and added to the above solution. The resulting suspension was stirred for 12 h at room temperature under nitrogen before quenching with 50 mL of methanol. The mixture was extracted with 1,2-dichloromethane (DCM). The combined organic phases were dried (MgSO_4). The crude product was then purified by column chromatography, resulting in the desired product in 55 % total yield. ¹H NMR (400 MHz, DMSO-d_6) δ : 8.52 (d, $J = 9.2$ Hz, 1H), 8.29–8.24 (m, 5H), 7.87 (d, $J = 8.4$ Hz, 2H), 7.63–7.55 (m, 3H), 7.52–7.48 (m, 2H), 7.39–7.36 (m, 2H). EI-MS (m/z): 320 (12%), 321 (78%), 322 (19%), 323 (2.5%).

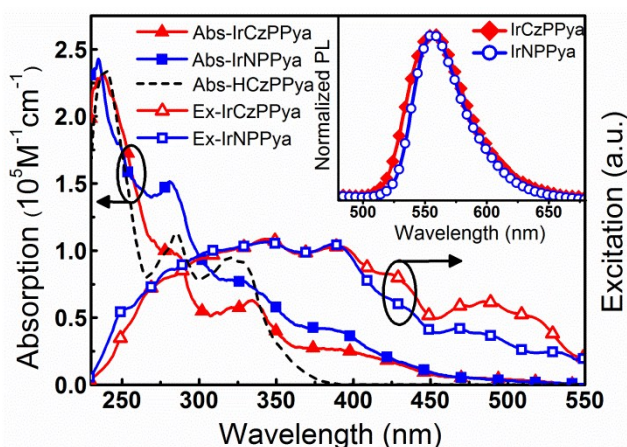


Fig. 1 Uv-visible, excitation (for 560 nm emission) and emission (inset) spectra for IrCzPPya, IrNPPya in DCM (about 1.0×10^{-5} M) at 298 K. The dashed line is a visual guide showing the HCZPPya ligand absorption (A.U.) in DCM.

2.1.2 Synthesis of diphenyl-(6-phenyl-pyridazin-3-yl)-amine (HNPPya)

Diphenyl-(6-phenyl-pyridazin-3-yl)-amine (HNPPya) was prepared following the above mentioned procedure. Yield: 49%. ^1H NMR (400 MHz, DMSO-d_6) δ : 8.00 (d, $J = 7.6$ Hz, 2H), 7.96 (d, $J = 9.2$ Hz, 1H), 7.51-7.47 (m, 2H), 7.44-7.39 (m, 5H), 7.25-7.21 (m, 6H), 7.00 (d, $J = 9.2$ Hz, 1H). EI-MS (m/z): 321 (2%), 322 (100%), 323 (27%), 324 (4%).

2.1.3 Synthesis of tris[9-(6-phenylpyridazin-3-yl)-9H-carbazole]iridium(III) (IrCzPPya)

Starting materials HCZPPya (126 mg, 0.4 mmol) and Ir(acac)₃ (48 mg, 0.1 mmol) were dissolved in degassed glycerol (6 mL). The reaction mixture was refluxed under nitrogen environment for 12 h, and then cooled to room temperature, water was added and the mixture was extracted with DCM. The organic layer was dried over MgSO_4 , and evaporated to dryness. The crude product was then purified by flash chromatography with a silica gel column. Finally orange colored product was obtained in 80% yield. ^1H -NMR (400MHz, DMSO-d_6) δ : 8.77 (d, $J = 9.4$ Hz, 3H), 8.02 (d, $J = 7.9$ Hz, 3H), 7.94-7.79 (m, 9H), 7.11-6.85 (m, 21H), 6.76 (t, $J = 7.7$ Hz, 6H). ^{13}C NMR (100 MHz, DMSO-d_6) δ : 164.99, 160.69, 152.77, 141.63, 138.3, 137.38, 132.27, 130.64, 129.39, 126.83, 126.43, 125.6, 123.91, 121.45, 120.29, 111.2. MALDI-TOF MS (m/z): Calcd. for $\text{C}_{66}\text{H}_{42}\text{N}_9\text{Ir}$: 1152, Found: 1153 ($[\text{M}^+ + \text{H}]$). Anal. Calcd. for $\text{C}_{66}\text{H}_{42}\text{N}_9\text{Ir}$: C, 68.88; H, 3.57; N, 10.98. Found: C, 68.75; H, 3.64; N, 10.94.

2.1.4 Synthesis of tris(N,N,6-triphenylpyridazin-3-amine)iridium(III) (IrNPPya)

Tris(N,N,6-triphenylpyridazin-3-amine)iridium(III) (IrNPPya) was prepared by the reaction of above mentioned procedure. ^1H -NMR (400MHz, DMSO-d_6) δ : 7.90 (d, $J = 9.4$ Hz 3H), 7.63 (d, $J = 7.8$ Hz, 3H), 7.25 (t, $J = 7.5$ Hz 12H), 7.05 (t, $J = 7.3$ Hz 6H), 6.86-6.66 (m, 21H), 6.43 (d, $J = 9.3$ Hz, 3H). ^{13}C NMR (100 MHz, DMSO-d_6) δ : 160.74, 157.8, 144.74, 142.74, 138.31, 136.61,

129.73, 28.82, 125.64, 125.02, 123.91, 123.61, 120.16, 118.42. MALDI-TOF MS (m/z): Calcd. for $\text{C}_{66}\text{H}_{48}\text{N}_9\text{Ir}$: 1158, Found: 1159 ($[\text{M}^+ + \text{H}]$). Anal. Calcd. for $\text{C}_{66}\text{H}_{48}\text{N}_9\text{Ir}$: C, 68.50; H, 4.11; N, 10.90. Found: C, 68.57; H, 4.15; N, 10.91.

2.2 Device fabrication and characterization

The indium tin oxide (ITO) coated glass with sheet resistance of $15 \Omega \text{ Square}^{-1}$ was used as the starting substrate. Before used in device, ITO glass substrates were precleaned carefully with deionized water, acetone, and ethanol, then treated with O_2 plasma for 30 seconds. All layers were grown in succession by thermal evaporation without breaking vacuum (1.0×10^{-4} Pa). All organic materials, except for dopants, were deposited at a rate of 2.0 \AA s^{-1} . After evaporation the devices were removed from the vacuum deposition chamber, the current-luminance-power characteristics and EL spectra of the devices were measured with a computer-controlled DC power supply and a PR655 photometer at room temperature. Emission area of the devices was 0.1 cm^2 as defined by the overlapping area of the anode and the cathode.

3 Results and discussion

3.1 Photophysical properties

Fig. 1 depicts the UV-vis absorption, excitation and emission (inset) spectra of IrCzPPya and IrNPPya in DCM. The two complexes show similar spectral features, reflecting their structural similarity. In terms of absorption, the strong peaks below 350 nm are assigned to the spin-allowed $^1\pi\pi^*$ transition of the cyclometalated ligands. This is in agreement with the absorption of free ligand HCZPPya, which presents no peaks above 350 nm (Fig. 1, dashed line). The shoulder of 377-380 nm can be ascribed to a typical spin-allowed metal to ligand charge transfer transition ($^1\text{MLCT}$). And the absorption after 380 nm is attributed to both spin-orbit coupling enhanced $^3\pi\pi^*$ and $^3\text{MLCT}$ transitions. Compared to IrCzPPya, absorption from IrNPPya is stronger, inferring its higher exciton forming efficiency in optical mode, which may benefit exciton generation in carrier injection mode such as OLED. The excitation spectra of IrCzPPya and IrNPPya monitored at emission of 560 nm do not resemble their absorption spectra, as shown in Fig. 1. The more intensive excitation spectrum in the wavelength region greater than 350 nm indicates more contribution of exciton in this region to the phosphorescence though the absorption in this region is smaller. This is understandable because besides excitons formed by direct absorption, those by intersystem crossing (ISC) from singlet also contribute to phosphorescence. Both IrCzPPya and IrNPPya exhibit strong orange photoluminescence with peaks of 556 nm and 558 nm, respectively. Their broad and structureless feature indicates that the emissions are MLCT dominated.

The photoluminescence (PL) quantum yields (Φ_{PL}) of the two new complexes were determined to be 0.45 and 0.55 for IrCzPPya and IrNPPya, respectively, measured in degassed DCM solution using Ir(ppy)₃ (assumed as 1.00) as standard.³⁰⁻³² The excited-state decay of the complexes are single-exponential, with observed lifetime (τ_{ph}) of 4.0 μs and 6.0 μs , for IrCzPPya and IrNPPya, respectively. It seems abnormal that IrCzPPya possesses lower Φ_{PL} (0.45) and shorter τ_{ph} (4.0 μs), since molecu-

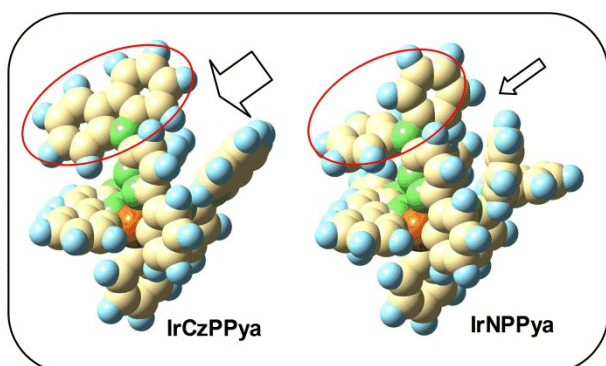


Fig. 2 DFT optimized geometries of IrCzPPya and IrNPPya molecules, the elliptic circles indicate carbazole or diphenylamine group

les with a more rigid structure such as carbazole tend to exhibit higher Φ_{PL} . DFT (density functional theory) calculation may shed light on this. As can be seen from the optimized molecule geometry (Fig. 2), the more rigid structure of carbazole moiety in IrCzPPya renders an increased available space for the penetration of environmental species compared to diphenylamine moiety in IrNPPya. Thus in IrCzPPya the channel for accessing the core part of the complex (i.e., Ir-C or Ir-N bonding) is larger, leading to more severe deactivation of MLCT process hence reducing τ_{ph} and Φ_{PL} .

3.2 Electrochemical and thermal properties

The electrochemical properties of IrCzPPya and IrNPPya were probed by cyclic voltammetry (CV). Both compounds exhibit reversible oxidation process in DCM solution. According to the oxidation potentials (Fig. S3 and S4), the HOMOs (the highest occupied molecular orbitals) of IrCzPPya and IrNPPya were calculated to be -5.70 eV and -5.40 eV, respectively. Subsequently, the corresponding LUMOs (the lowest unoccupied molecular orbitals) were estimated to be -3.10 eV for IrCzPPya and -2.80 eV for IrNPPya, referring to their HOMOs and absorption spectra.^{30,33} These values are summarized in table S1, which are helpful to design the structure of PhOLEDs and WOLED based on the new iridium complexes.

Thermal gravimetric analysis (TGA) showed that the two compounds exhibited good thermal stabilities. A weight loss of 5% was found at temperatures of 426 and 382 °C for IrCzPPya and IrNPPya, respectively (Fig. S5 and S6). Similar to our previous report about C^N=N type iridium complexes,^{9,16} this good thermal stability should be ascribed to the strong Ir-N bonding due to the lack of steric hindrance between Ir and N atoms, in which the coordinating N is adjacent to another N atom with only a pair of lone electrons.

3.3 Electrophosphorescent devices

To examine the potential usage of these materials as emitters in PhOLED, monochromic devices were fabricated with the traditional structure of ITO/NPB [N,N'-bis-(1-naphthyl)-N,N'-diphenyl,1,1'-biphenyl-4,4'-diamine] (40 nm)/6% phosphor doped CBP [4,4'-bis(carbazol-9-yl)biphenyl] (20 nm)/BCP [2,9-dimethyl-4,7-diphenyl-1,10-phenanthroline] (8 nm)/Alq [tris(8-

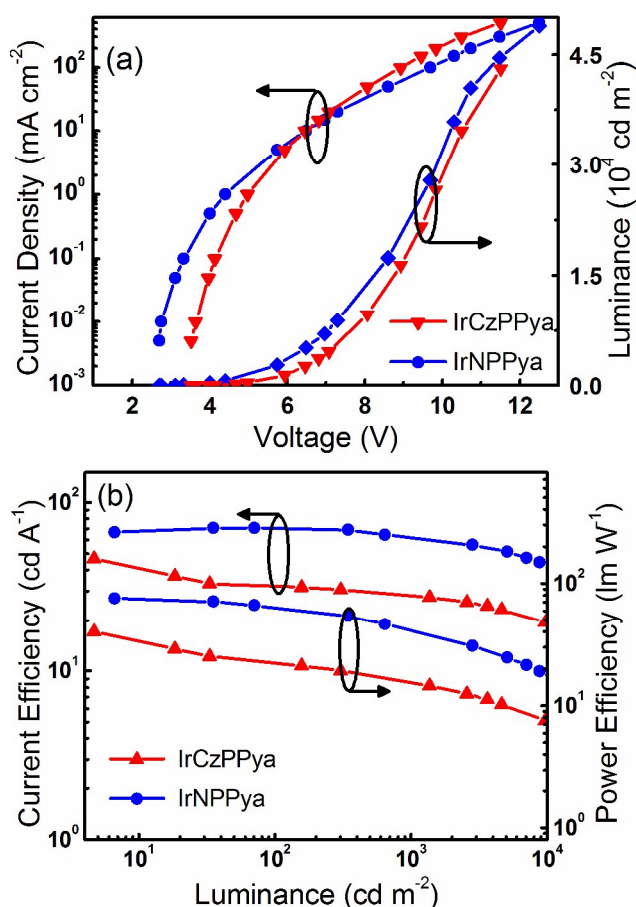


Fig. 3 (a) $I-V-L$ Current density-Voltage-Luminance curves and (b) Efficiencies of orange PhOLED devices.

hydroxyquinolinato)aluminum(HH m)] (20 nm)/LiF (1 nm)/Al (100 nm). Here, NPB acts as the hole-transporting layer (HTL), CBP acts as the triplet host, BCP is the hole-blocking layer and Alq is the electron-transporting layer. As shown in Fig. 3a, these devices show low driving voltages, which should be partially due to the improved electrical property of the iridium complexes with hole transport moiety. At the same driving voltage, the current density of IrNPPya device is higher than IrCzPPya device, inferring its better conductivity. It should be noticed that the electricity in IrCzPPya based device improves with driving voltage, reaching and even exceeding that in IrNPPya device at high electric field. This can be attributed to the electric field induced conformation change in materials bearing carbazole group, which alters material conductivity.³⁴ Both devices exhibit strong orange EL with emission peaks of 556 and 564 nm (Fig. S7 and S8), and turn on voltages of 3.5 and 2.7 V for IrCzPPya and IrNPPya, respectively. The IrNPPya device shows a maximum efficiency of 70.8 cd A^{-1} (75.4 lm W^{-1} , 30.8%) (Fig. 3b). At a brightness of 1000 cd m^{-2} , the efficiencies are still as high as 63.3 cd A^{-1} (43.5 lm W^{-1} , 21.8%), showing extremely low efficiency roll-off. This is among the state-of-the-art results reported to date for orange PhOLEDs with similar wavelength.^{35,36} The IrCzPPya device shows lower performance with peak efficiencies of 46.1 cd A^{-1} , 40.1 lm W^{-1} , 22.6%. As discussed previously, compared to IrNPPya, IrCzPPya exhibits weaker absorption and lower Φ_{PL} ,

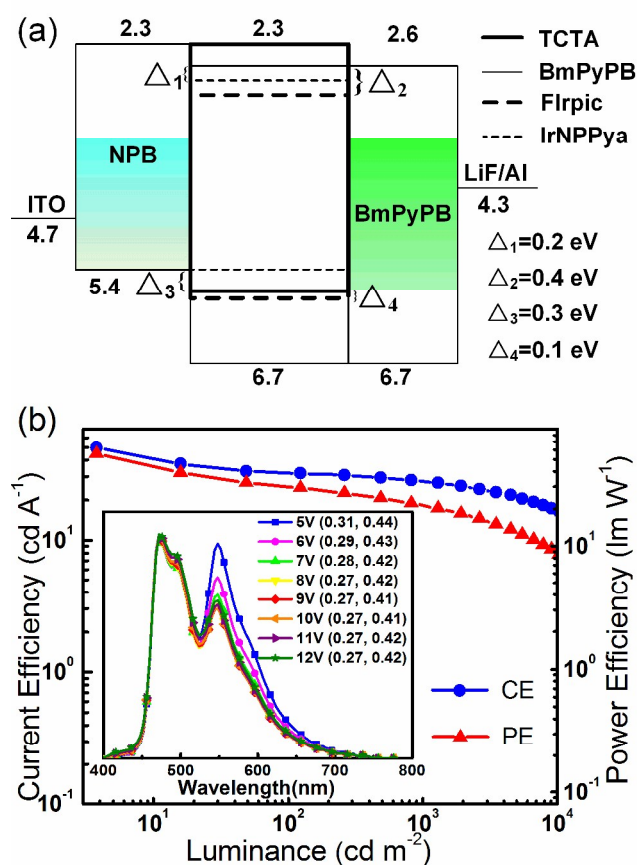


Fig. 4 (a) Device structure of the WOLED; (b) Efficiencies of WOLED device, the inset is the normalized EL spectra of WOLED at voltage of 4-12 V.

which should partially account for its relatively low device performance. On the other hand, due to the zero hole injection barrier from NPB to IrNPPya, good hole-trapping in IrNPPya can be realized, leading to enhanced opportunity for direct exciton formation in IrNPPya, which is beneficial to the electrophosphorescence in IrNPPya device (see Fig. 4a).

Inspired by the ultra-high efficiency of IrNPPya device, we further prepared WOLED employing IrNPPya as orange emission element in combination with the traditional blue phosphor FIrpic. The device structure is ITO/NPB(45 nm)/TCTA:BmPyPB:FIrpic:IrNPPya (4:1, 10 wt%, 0.8 wt%, 20 nm)/BmPyPB(40nm)/LiF/Al. Significantly, this device contains single EML with only three organic layers (shown in Fig. 4a). Here, the extremely low concentration of orange phosphor (0.8%) was employed for the purpose of reducing/avoiding the quenching of the blue emission in the WOLED. TCTA and BmPyPB with ratio of 4:1 were used as cohost to enable bipolar transport in the EML. This cohost almost perfectly matches the adjacent hole transport layer of NPB and the electron transport layer of BmPyPB, with barrier of 0.3 eV (Δ_3) for hole and 0.0 eV for electron injections, facilitating carrier injection into the EML. Device performances are listed in Table 1 and shown in Fig. 4b. As can be seen from Fig. 4b, the EL spectra contain two emission peaks of 472 nm and 548 nm with comparable intensity, which

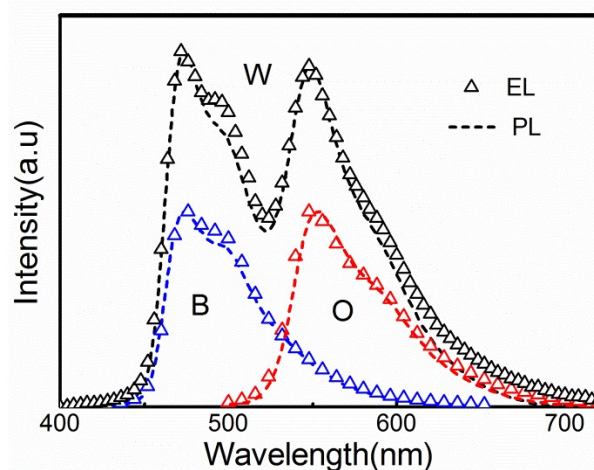


Fig. 5 The EL spectra of the white (W), blue (B) and orange (O) OLED devices, and the PLs of corresponding EML films: TCTA:BmPyPB:FIrpic:IrNPPya (4:1, 10%, 0.8%) for white, TCTA:BmPyPB:FIrpic (4:1, 10%) for blue, and TCTA:BmPyPB: IrNPPya (4:1, 0.8%) for orange.

can be assigned to the emission from FIrpic and IrNPPya, respectively. Besides, the color stability can also be seen in the insert figure of Fig. 4b. For example, increasing the driving voltage from 4 V to 12 V, the CIE coordinates change from (0.33, 0.46) to (0.27, 0.42), with relatively small variation of (0.06, 0.04) among single EML WOLED.⁴⁷⁻²³ The maximum efficiencies of the WOLED are 55.9 lm W⁻¹, 49.9 cd A⁻¹, and 23.9%. As seen in Table 1, compared to the most advanced WOLEDs, our white device reveals a superior trade-off among simplicity/efficiency/CIE-coordinate factors that are critical for commercialization. Specifically, in terms of similar CIE coordinates at practically useful luminance of 1000 cd m⁻² and WOLEDs employing single EML, the efficiencies of our device (21.4 lm W⁻¹ and 27.7 cd A⁻¹) are among the best.⁴⁷⁻²³

To investigate the dominate mechanism for our single EML WOLED with only three organic layers, we constructed two monochromic devices by keeping the device structure the same as the WOLED except that either FIrpic or IrNPPya was removed. The film PLs of the corresponding EMLs were also studied. Both FIrpic and IrNPPya based monochromic devices exhibit very high efficiencies, e.g., the maximum values are 29.0 cd A⁻¹/32.5 lm W⁻¹/16.8% and 57.9 cd A⁻¹/60.6 lm W⁻¹/23.8% for FIrpic and IrNPPya devices, respectively. Compared to 6% IrNPPya device (see Table 1), the low doping concentration device with 0.8% IrNPPya shows larger roll-off mainly due to more severe triplet excitons quenching, because when the current density increases exciton density increases more dramatically in device with such low phosphor concentration. As shown in Fig. 5, the ELs of the monochromic and the white devices exactly match the corresponding PLs, inferring that these ELs are solely from the corresponding phosphors, no exciplex or electropex involved, and both FIrpic and IrNPPya are perfectly fitted with the bipolar cohost, which rendering the high efficiency of the two monochromic as well as the white devices. Further evidence can be got by examining the energy levels in Fig. 4a. As well known, the favorable hole/electron trap requires the HOMO/LUMO level

Table 1. Most advanced, selected performance characteristics of WOLEDs with single EML and our orange EL.

Reference (Reported Year)	$V_{\text{turn-on}}$ [V]	$\eta_{\text{power}} @ \text{Max}/1000$ cd m^{-2} [lm W^{-1}]	$\eta_{\text{current}} @ \text{Max}/1000$ cd m^{-2} [cd A^{-1}]	$\text{EQE} @ \text{Max}/1000$ cd m^{-2} [%]	Total emitter(s) /Organic layers	$\text{CIE}[x, y] @ 1000$ cd m^{-2}
[23a] (2012)	2.4	67.2/33.5	53.5/42.6	26.6/21.2	2/4	(0.46, 0.44) @100 cd m^{-2}
[23b] (2013)	NA ^{a)}	59.8/31.3 (Total) ^{b)}	57.2/40.6 (Total) ^{b)}	24.7/18.3(Total) ^{b)}	2/4	(0.41, 0.46)
[23c] (2014)	3.3	60.4/27.4	62.5/49.9	22.9/NA	2/5	(0.39, 0.45)
[23d] (2013)	NA ^{a)}	63.2/50.1	77.0/72.8	24.0/22.8	2/4	(0.38,0.49) @5 mA cm^{-2}
[23e] (2012)	>3	47.6/23.3	70.6/44.3	26.0/16.4	2/3	(0.38, 0.43)
[23f] (2014)	NA ^{a)}	55.7/24.0	NA ^{a)/NA^{a)}}	21.5/17.7	1/6	(0.37, 0.42)
[23g] (2014)	NA ^{a)}	69.4/55.0	76.2/73.6	24.6/23.6	2/4	(0.36, 0.48)@4V
This work ^{c)}	2.9	55.9/21.4	49.9/27.7	23.9/9.7	2/3	(0.33, 0.46)
6%IrNPPya ^{d)}	2.7	75.4/43.5	70.8/63.3	30.8/21.8	1/4	(0.51, 0.49)
0.8% IrNPPya ^{d)}	2.9	60.6/12.0	57.9/18.0	23.8/5.2	1/3	(0.44, 0.54)

^{a)} Not available from reference; ^{b)} Total stands for total efficiency; ^{c)} White OLED; ^{d)} Orange EL

of the dopant locate above/below that of the host. From Fig. 4a, it can be seen that, with this cohost, both the orange phosphor and the blue phosphor can trap electron, with favorable energy of $\Delta_1=0.2$ eV, $\Delta_2=0.4$ eV, respectively. For IrNPPya, besides the effective electron trapping, there is another benefit arising from the device structure, i.e., no hole injection barrier exists from NPB to IrNPPya, thus both electron (from BmPyPB) and hole (from TCTA and NPB) can be trapped easily and direct exciton formation on IrNPPya is dominated. A direct charge recombination on the molecular sites of phosphorescent dyes will reduce the host-guest exchange energy loss, benefiting to device power efficiency.^{13, 17, 13, 23f}

4 Conclusions

In summary, we have synthesized two new strong orange-emission and thermally stable iridium complexes (IrNPPya, IrCzPPya) of C[^]N=N type ligand containing diphenylamine or carbazole. As disclosed by DFT simulation, compared to IrNPPya, the rigid structure of carbazole in IrCzPPya renders an increased available space for the penetration of environmental species, reducing τ_{ph} and Φ_{PL} . Additionally, owing to the electron-rich and hole-transport features of amine and carbazole moieties, electrical property of these complexes are expected to improve, which would benefit to device performance. Using IrNPPya (IrCzPPya) as the dopant emitter, the device shows maximum efficiencies of 70.8 cd A^{-1} (46.1 cd A^{-1}), 75.4 lm W^{-1} (40.1 lm W^{-1}) and 30.8% (22.6%). Particularly, the roll-offs of these devices are very low. For instance, in IrNPPya based device, the efficiencies are still as high as 63.3 cd A^{-1} (43.5 lm W^{-1} , 21.8%) at a brightness of 1000 cd m^{-2} . This is among the state-of-the-art results reported to date for orange PhOLEDs with similar wavelength. Combining IrNPPya with the blue emitter FIrpic, the quadri-deposited single-EML WOLED with high efficiency and

good CIE has been successfully constructed. Maximum efficiencies of 55.9 lm W^{-1} , 49.9 cd A^{-1} , and 23.9% with CIE coordinates of (0.33, 0.46) are achieved, which are among the best WOLEDs with similar CIE coordinates. The good performance in this single EML WOLED mainly owes to the energetically matched material system containing a bipolar cohost and a new iridium complex, in coupled with the strong intrinsic emission of the new phosphor. In such a device configuration, besides hole and electron balance in the EML, direct charge trapping on FIrpic and IrNPPya molecules can be efficiently realized. Furthermore, the low doping concentration (0.8%) of IrNPPya will reduce/block energy transfer from the blue phosphor thus guaranteeing its emission in the WOLED. All of these enable efficient emission from both phosphors, leading to rather good quality of white color. Our work further proves that high-efficiency WOLEDs could be obtained by single-EML device structure using a doping concentration regulation strategy and employing a suitable material system with well matched energy levels.

Acknowledgements

This work was financially supported by the National Natural Science Foundation of China (Nos. 61077021, 61076016, 61474064), Nanjing University of Posts and Telecommunications (Nos. NY212076, NY212050), National Basic Research Program of China 973 Program (2015CB932200), the Ministry of Education of China (IRT1148), the Priority Academic Program Development of Jiangsu Higher Education Institutions (PAPD:YX03001), and the Synergistic Innovation Center for Organic Electronics and Information Displays.

Notes and references

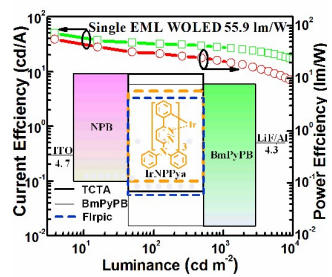
^a Key Laboratory for Organic Electronics and Information Displays & Institute of Advanced Materials (IAM), Jiangsu National Synergistic Innovation Center for Advanced Materials (SICAM), Nanjing University of Posts & Telecommunications, 9 Wenyuan Road, Nanjing 210023, China. E-mail: iamxbmi@njupt.edu.cn

^b School of Material Science and Engineering, Jiangsu Engineering Centre for Flat-Panel Displays & Solid-state Lighting, Nanjing University of Posts & Telecommunications, 9 Wenyuan Road, Nanjing 210023, China. E-mail: iamzqgao@njupt.edu.cn

† Electronic Supplementary Information (ESI) available: [Photophysical, thermal, electrochemical properties and EL spectra of IrNPPya and IrCzPPya]. See DOI: 10.1039/b000000x/

‡ These authors contributed equally to this work.

- 1 L. Xiao, Z. Chen, B. Qu, J. Luo, S. Kong, Q. Gong and J. Kido, *Adv. Mater.*, 2011, **23**, 926.
- 2 G. J. McGraw and S. R. Forrest, *Adv. Mater.*, 2013, **25**, 1583.
- 3 H. Sasabe and J. Kido, *J. Mater. Chem. C.*, 2013, **1**, 1699.
- 4 M. A. Baldo, D. F. O'Brien, Y. You, A. Shoustikov, S. Sibley, M. E. Thompson and S. R. Forrest, 1998, *Nature*, **395**, 151.
- 5 D. Tanaka, H. Sasabe, Y. J. Li, S. J. Su, T. Takeda and K. Junji, *Jpn. J. Appl. Phys.*, 2007, **46**, L10.
- 6 K. Udagawa, H. Sasabe, C. Cai and J. Kido, *Adv. Mater.*, 2014, **26**, 5062.
- 7 K. H. Kim, C. K. Moon, J. H. Lee, S. Y. Kim and J. J. Kim, *Adv. Mater.*, 2014, **26**, 3844.
- 8 T. Giridhar, W. Cho, Y. H. Kim, T. H. Han, T. W. Lee and S. H. Jin, *J. Mater. Chem. C.*, 2014, **2**, 9398.
- 9 B. X. Mi, P. F. Wang, Z. Q. Gao, C. S. Lee, S. T. Lee, H. L. Hong, X. M. Chen, M. S. Wong, P. F. Xia, K. W. Cheah, C. H. Chen and W. Huang, *Adv. Mater.*, 2009, **21**, 339.
- 10 D. Liu, H. Ren, L. Deng and T. Zhang, *ACS Appl. Mater. Interfaces*, 2013, **5**, 4937.
- 11 H. H. Chou, Y. K. Li, Y. H. Chen, C. C. Chang, C. Y. Liao and C. H. Cheng, *ACS Appl. Mater. Interfaces*, 2013, **5**, 6168.
- 12 H. Cao, G. Shan, X. Wen, H. Sun, Z. Su, R. Zhong, W. Xie, P. Li and D. Zhu, *J. Mater. Chem. C.*, 2013, **1**, 7371.
- 13 B. Zhang, G. Tan, C. S. Lam, B. Yao, C. L. Ho, L. Liu, Z. Xie, W. Y. Wong, J. Ding and L. Wang, *Adv. Mater.*, 2012, **24**, 1873.
- 14 Z. Q. Gao, B. X. Mi, H. L. Tam, K. W. Cheah, C. H. Chen, M. S. Wong, S. T. Lee and C. S. Lee, *Adv. Mater.*, 2008, **20**, 774.
- 15 C. Liu, L. Mao, H. X. Jia, Z. J. Liao, H. J. Wang, B. X. Mi and Z. Q. Gao, *Sci. China. Chem.*, 2014, **1**.
- 16 Z. J. Liao, T. J. Zhu, B. X. Mi, Z. Q. Gao, Q. L. Fan and W. Huang, *Prog. Chem.*, 2011, **23**, 1627.
- 17 B. Tong, Q. Mei, S. Wang, Y. Fang, Y. Meng and B. Wang, *J. Mater. Chem.*, 2008, **18**, 1636.
- 18 Y. Fang, B. Tong, S. Hu, S. Wang, Y. Meng, J. Peng and B. Wang, *Org. Electron.*, 2009, **10**, 618.
- 19 Q. Mei, L. Wang, B. Tian, B. Tong, J. Weng, B. Zhang, Y. Jiang and W. Huang, *Dyes and Pigment.*, 2013, **97**, 43.
- 20 L. Shi, J. Su and Z. Wu, *Inorg. Chem.*, 2011, **50**, 5477.
- 21 L. Y. Guo, X. L. Zhang, M. J. Zhuo, C. Liu, W. Y. Chen, B. X. Mi, J. Song, Y. H. Li and Z. Q. Gao, *Org. Electron.*, 2014, **15**, 2964.
- 22 S. J. Su, E. Gonmori, H. Sasabe and J. Kido, *Adv. Mater.*, 2008, **20**, 4189.
- 23 a) J. Ye, C. J. Zheng, X. M. Ou, X. H. Zhang, M. K. Fung and C. S. Lee, *Adv. Mater.*, 2012, **24**, 3410; b) X. K. Liu, C. J. Zheng, M. F. Lo, J. Xiao, Z. Chen, C. L. Liu, C. S. Lee, M. K. Fung and X. H. Zhang, *Chem. Mater.*, 2013, **25**, 4454; c) B. Pan, B. Wang, Y. Wang, P. Xu, L. Wang, J. Chen and D. Ma, *J. Mater. Chem.*, 2014, **2**, 2466; d) S. C. Dong, Y. Liu, Q. Li, L. S. Cui, H. Chen, Z. Q. Jiang and L. S. Liao, *J. Mater. Chem. C.*, 2013, **1**, 6575; e) B. Zhang, G. Tan, C. S. Lam, B. Yao, C. L. Ho, L. Liu, Z. Xie, W. Y. Wong and J. Ding, L. Wang, *Adv. Mater.*, 2012, **24**, 1873; f) G. Li, T. Fleetham and J. Li, *Adv. Mater.*, 2014, **26**, 2931; g) L. S. Cui, Y. Liu, Q. Li, Z. Q. Jiang and L. S. Liao, *Org. Electron.*, 2014, **15**, 1368.
- 24 W. Zhang, H. M. Cho and J. S. Moore, *Org. Synth.*, 2007, **84**, 177.
- 25 T. Shibahara and M. Yamasaki, *Inorg. Chem.*, 1991, **30**, 1687.
- 26 S. Jung, Y. Kang, H. S. Kim, Y. H. Kim, C. L. Lee, J. J. Kim, S. K. Lee and S. K. Kwon, *Eur. J. Inorg. Chem.*, 2004, **17**, 3415.
- 27 A. B. Tamayo, B. D. Alleyne, P. I. Djurovich, S. Lamansky, I. Tsyba, N. N. Ho, R. Bau and M. E. Thompson, *J. Am. Chem. Soc.*, 2003, **125**, 7377.
- 28 Vivian W. W. Yam, B. Li, Y. Yang, Ben W. K. Chu, Keith M. C. Wong and K. K. Cheung, *Eur. J. Inorg. Chem.*, 2003, **22**, 4035.
- 29 M. K. Leung, Y. H. Hsieh, T. Y. Kuo, P. T. Chou, J. H. Lee, T. L. Chiu and H. J. Chen, *Org. Lett.*, 2013, **15**, 4694.
- 30 D. Xia, B. Wang, B. Chen, S. Wang, B. Zhang, J. Ding, L. Wang, X. Jing and F. Wang, *Angew. Chem. Int. Ed.*, 2014, **53**, 1048.
- 31 V. N. Kozhevnikov, Y. Zheng, M. Clough, H. A. Al. Attar, G. C. Griffiths, K. Abdullah, S. Raisys, V. Jankus, M. R. Bryce and A. P. Monkman, *Chem. Mater.*, 2013, **25**, 2352.
- 32 Q. L. Xu, C. C. Wang, T. Y. Li, M. Y. Teng, S. Zhang, Y. M. Jing, X. Yang, W. N. Li, C. Lin, Y. X. Zheng, J. L. Zuo and X. Z. You, *Inorg. Chem.*, 2013, **52**, 4916.
- 33 S. Lee, S. O. Kim, H. Shin, H. J. Yun, K. Yang, S. K. Kwon, J. J. Kim, Y. H. Kim, *J. Am. Chem. Soc.* 2013, **135**, 14321.
- 34 L. H. Xie, Q. D. Ling, X. Y. Hou and W. Huang, *J. Am. Chem. Soc.*, 2008, **130**, 2120.
- 35 J. H. Jou, Y. X. Lin, S. H. Peng, C. J. Li, Y. M. Yang, C. L. Chin, J. J. Shyue, S. S. Sun, M. Lee, C. T. Chen, M. C. Liu, C. C. Chen, G. Y. Chen, J. H. Wu, C. H. Li, C. F. Sung, M. J. Lee and J. P. Hu, *Adv. Funct. Mater.*, 2014, **24**, 555.
- 36 R. Wang, L. Deng, T. Zhang and J. Li, *Dalton Trans.*, 2012, **41**, 6833.



Two new iridium complexes were prepared. With one of them, both high efficiencies orange EL and single-EML WOLED were constructed.